DMD Fast Forward. Published on March 18, 2005 as doi:10.1124/dmd.104.002568




# Impact of Endotoxin-Induced Changes in P-Glycoprotein Expression on Disposition of Doxorubicin in Mice.

Georgy Hartmann
Vessela Vassileva
Micheline Piquette-Miller

Leslie Dan Faculty of Pharmacy, University of Toronto
Toronto, Ontario, Canada (GH, VV, MPM)

Running title:

Altered Pharmacokinetics of DOX in Endotoxin-treated Mice

Corresponding Author:

Micheline Piquette-Miller, Ph.D.
Leslie Dan Faculty of Pharmacy, University of Toronto
19 Russell Street, Toronto ON M5S 2S2, Canada
Phone: (416) 946-3057
Fax: (416) 978-8511
E-mail: m.piquette.miller@utoronto.ca

Number of text pages: 37
Number of tables: 4
Number of figures: 5
Number of references: 34
Number of words in Abstract: 251
Number of words in Introduction: 616
Number of words in Discussion: 1453

**List of Abbreviations**

| | |
|---|---|
| AUC | area under the plasma concentration time curve |
| Bsep | Bile salt export pump |
| HPLC | high performance liquid chromatography |
| LPS | lipopolysaccharide (bacterial endotoxin) |
| M1 | metabolite 1 (doxorubicinol) |
| M2 | metabolite 2 (7-Deoxy-doxorubicinone) |
| M3 | metabolite 3 (7-Deoxy-doxorubicinolone) |
| *Mdr1* | multidrug resistance gene |

## ABSTRACT

P-glycoprotein (PGP) encoded by the *Mdr1* gene mediates the excretion of drugs in organs such as the liver and kidney. Inflammation has been shown to suppress the expression and activity of PGP in rodent liver, thus potentially altering the pharmacokinetics of drugs that are substrates of PGP. Here we examined the effect of endotoxin (LPS)-induced inflammation on the disposition of the PGP substrate doxorubicin (DOX) in the mouse. Male CD-1 mice received 5 mg/kg LPS intraperitoneally. DOX (5 mg/kg) was administered intravenously 24 h following LPS treatment. The time-course of DOX levels in plasma, urine, bile and tissues were analyzed by high performance liquid chromatography. PGP protein and mRNA expression in liver and kidney was measured using Western blots and reverse transcriptase polymerase chain reaction. As compared to controls, LPS-treated mice exhibited a significant decrease (50%) in biliary clearance, and 3-fold increased renal clearance of DOX. These changes were associated with strongly reduced PGP protein levels (30% Controls, $p<0.05$) in the liver, and increased PGP levels in the kidney (140% Controls, $p<0.05$). Hepatic mRNA levels of all *Mdr* isoforms were reduced in LPS-treated mice whereas renal *Mdr1b* levels were induced. In LPS-treated mice we also measured an increased area under the plasma concentration-time curve and reduced systemic clearance of DOX, as well as two- to five-fold increase in the urinary excretion of the doxorubicin and doxorubicinol aglycones. Our data suggest that endotoxin-induced inflammation in mice causes differential regulation of PGP in liver and kidney, thereby altering the clearance profile of DOX.

DMD Fast Forward. Published on March 18, 2005 as DOI: 10.1124/dmd.104.002568
This article has not been copyedited and formatted. The final version may differ from this version.



The cytochromes P450 and drug-transporting membrane proteins play an important role in the disposition and clearance of drugs. The drug transporter P-glycoprotein (PGP) is of particular clinical relevance because of its broad substrate specificity, which includes a variety of commonly used antineoplastic drugs, such as doxorubicin, vincristine, and paclitaxel. PGP is an ATP-dependent efflux pump encoded by the *Mdr1* (*Abcb1*) gene, and is expressed in tissues that mediate the excretion of drugs (liver, kidney), or that limit the entry of drugs into the body (intestine, blood-brain barrier). In mice, PGP exists in two isoforms, *Mdr1a* and *Mdr1b*. Experiments in knockout mice have demonstrated that the absence of one or both transporter isoforms greatly enhances the sensitivity to drugs, and can lead to drug toxicity not observed in wild-type animals (Borst and Schinkel, 1997).

Despite the physiological significance of PGP, many aspects regarding its cellular and molecular regulation still remain unclear. Whereas PGP is often overexpressed in cancer cells (thus rendering them resistant to cancer chemotherapy), inflammatory disease states such as endotoxemia are associated with suppression of PGP and other hepatic transporters (Piquette-Miller et al., 1998; Trauner et al., 1998). In rat and mouse models of experimentally induced inflammation, our group has previously shown that the expression and functional activity of PGP is reduced during acute inflammation, which is mediated primarily through the action of pro-inflammatory cytokines (Hartmann et al., 2001).

Moreover, several studies since the 1980s have shown that the pharmacokinetics of many drugs are altered in inflammation (Schneider and Bishop, 1982). Since acute inflammatory responses are chiefly mediated by the liver, this effect is most prominent for drugs that are cleared mainly by the liver, such as the β-adrenoreceptor antagonists (Piquette-Miller and Jamali, 1995). It is generally felt that suppression of the hepatic cytochrome P450 enzymes is a key factor that contributes to decreased hepatic clearance of drugs. However the significance of changes in the expression of hepatic transporters such as PGP has largely been overlooked. It would be of clinical importance to investigate the impact of inflammation-mediated suppression of hepatic PGP on drug kinetics, in particular for drugs that are known for their inherent toxicity, such as anticancer agents.

In a mouse model of endotoxin-induced acute inflammation, we sought to delineate the impact of PGP downregulation on the *in vivo* disposition and clearance of the PGP substrate doxorubicin (DOX). DOX is an antitumor agent widely utilized for the treatment of various neoplastic diseases. DOX is taken up into cells via passive processes and is extensively distributed to liver, spleen, kidney, heart and small intestine after intravenous administration (Broggini et al., 1980). DOX is mainly cleared by biliary secretion which occurs via PGP (Van Asperen et al., 2000). Direct intestinal secretion also appears to be an important route of DOX clearance (Van Asperen et al., 2000). Generally, in mice less than 10 % of the administered dose is metabolized through non-P450 enzyme systems, the aldoketoreductase (carbonylreductase) and the microsomal reductive glycosidase (Loveless et al., 1978). Three metabolites have been identified in the mouse: doxorubicinol, 7-deoxy-doxorubicinolone, and 7-deoxy-doxorubicinone, also termed metabolites M1, M2, and M3, respectively (Van Asperen et al., 1999).

In this report we show that endotoxin treatment causes murine PGP to be differentially regulated in liver and kidney, which is associated with alterations in the biliary and renal elimination of DOX and its metabolites. Our observations support the existence of tissue-specific mechanisms, thus a defect of hepatic PGP function may possibly be counterbalanced by induction in other eliminating organs, such as the kidney. These findings have important implications for the *in vivo* regulation of drug transporters in inflammatory disease, and add to understanding the physiological response underlying the pharmacokinetic changes during acute phase conditions.

## METHODS

**Animals and Treatment.** Animal studies were conducted in accordance with the guidelines of the Canadian Council on Animal Care. Eight-week-old male CD-1 mice (25-35 g) were supplied by Charles River (St. Constant, QC). The animals were injected with 5 mg/kg intraperitoneal (i.p.) LPS (from *E. coli* serotype 055:B5, Sigma, St. Louis MO). Control mice received the equivalent volume of saline buffer. Pharmacokinetic studies and analysis of hepatic PGP protein were performed 24 h following the treatment.

**Analysis of PGP Protein Expression.** Four mice from each treatment group were sacrificed. Livers and kidneys were excised, snap-frozen in liquid nitrogen, and stored at -80 °C. Western Blot analysis with the C-219 antibody was performed on protein samples prepared by homogenization of livers (1.0-1.5 g) or kidneys (0.45-0.8 g) based on previously published methods (Hartmann et al., 2001). The levels of PGP protein expression are reported as percentages of average control values (n=4).

**RT-PCR Analysis of *Mdr* mRNA expression.** Total RNA was extracted from livers and from kidneys using the Amersham QuickPrep™ RNA extraction kit following manufacturer's instructions. Semiquantitative Reverse Transcription-Polymerase Chain Reaction (RT-PCR) analysis was performed as previously described (Hartmann et al., 2001). The optical densities (OD) of PCR products were normalized to 18 S ribosomal RNA (rRNA) band intensities. Levels of mRNA expression are reported as percentages of normalized values, as compared to control

values. Normalized values were calculated as ratios of (OD *Mdr* mRNA) / (OD 18 S rRNA). Results obtained from RT-PCR were later confirmed by real-time quantitative PCR.

***In Vivo* Pharmacokinetic Study of Doxorubicin.** Doxorubicin (DOX)-HCl (from ICN, Costa Mesa CA) was dissolved in saline to give a 1 mg/mL solution, and administered to mice i.v. into a lateral tail vein at a dose of 5 mg/kg. At various time points following injection (15 min, 30 min, 1 h, 2 h, 4 h, 8 h, 12 h, 24 h), three to five mice from each group were sacrificed. Blood samples were drawn from the inferior vena cava and collected in heparinized syringes. Tissue samples from liver, kidneys, intestines (including intestinal contents), brain and heart were collected. Blood samples were centrifuged for 10 min at 3000 × *g* and 4 ˚C to obtain plasma. For excretion experiments, mice were housed in Nalgene metabolic cages immediately following DOX administration. Urine and feces were collected in six-hour time intervals up to 24 h, starting at 6:00 PM. All plasma and tissue samples were frozen at -70 ˚C until analysis. Feces, urine and bile samples were stored at -20 ˚C.

For measurement of DOX biliary excretion, mice were anaesthetized with 60 mg/kg i.p. sodium pentobarbital. After opening the abdominal cavity, the lower part of the common bile duct (adjacent to the pancreas) was ligated and a micro-cannula (BioTime, Berkeley, CA) was inserted into the upper part of the bile duct approximately 3 mm below the branching site, and fixed with 5-0 silk suture. DOX-HCl at a dose of 5 mg/kg was injected into a tail vein. Bile was collected in pre-weighed 1.5 mL Eppendorf tubes in 20-minute time intervals for up to 80 minutes. During bile collection, the animals were maintained at 37 °C using a heat lamp, and the exposed abdominal tissues were moistened with saline to prevent dehydration. If required,

additional anaesthetic (up to 30 µl) was instilled directly into the abdominal cavity. Bile volumes were determined by weighing the tubes after bile collection and assuming a specific gravity of 1 g/mL bile.

**Doxorubicin HPLC Assay.** The extraction of DOX and metabolites from plasma, urine, feces, bile and tissue samples was performed according to the method of Van Asperen et al. (1998). Similarly, DOX concentrations in the samples were measured based on the HPLC method of Van Asperen et al. (1998), with minor modifications. Briefly, the HPLC system consisted of a Waters 600E system controller and pump, a Waters 715 Ultra-WISP autosampler, and a Perkin Elmer 500 fluorescent detector. Doxorubicin and the metabolites M1 (doxorubicinol), M2 (7-Deoxy-doxorubicinone) and M3 (7-Deoxy-doxorubicinolone) were separated on a Beckman Ultrasphere ODS 5 µm ($C_{18}$) column, 150 x 4.6 mm, preceded by a Waters µ-Bondapak $C_{18}$ guard column. A gradient elution was performed by mixing acetonitrile and water (pH 2.05) at a constant flow rate of 1.1 mL/min, establishing a stepwise gradient of 25-40 % acetonitrile from 0-25 min, followed by re-equilibration with 25 % acetonitrile. Fluorescent detection was achieved at an excitation wavelength of 460 nm and an emission wavelength of 550 nm. Peaks were recorded and integrated using a Waters SAT/IN2 data module and Waters Empower™ software. Calibration curves were obtained by least squares linear regression analysis of the concentration versus the ratio of peak area of doxorubicin, M1, M2, or M3 and the internal standard (I.S., daunorubicin, concentration 500 ng/mL). The intra-day and inter-day coefficients of variation were determined to be 7.2 % and 10.5 % (range: 0.01 to 5 µg/mL). The lower limit of quantitation was 2 ng/mL, using 200 µl of mouse plasma. The typical retention times recorded for DOX, M1, M2, M3 and I.S. were 6.3, 3.7, 18.4, 14.4 and 15.1 min, respectively.

The identity of the metabolites M1, M2 and M3 was determined by mass spectrometry (performed by ANALEST Laboratories, University of Toronto) and confirmed based on previously published mass spectra (Takanashi and Bachur, 1976). As internal standards for the doxorubicin metabolites were not available, the levels of metabolites were calculated as DOX equivalents of ng/mL (plasma, urine), or μg/g (tissue, bile). M1 was detected in urine but was not detectable in plasma. With the exception of heart, reliable data could not be obtained for M1 from homogenized tissues, due to interference with several endogenous peaks at early retention times.

**Plasma Binding Determination.** The plasma unbound fractions ($f_{u,plasma}$) of DOX in normal and endotoxemic mice was measured based on ultrafiltration method reported by Mayer and St-Onge (1995) with modifications. Briefly, mouse plasma samples were spiked with DOX 10 μg/mL, and incubated at 37 °C for 30 min. Samples ( 200 μL) were then loaded onto Microcon-30 devices and centrifuged at 8000xg, 37°C for 10 min. Approximately 50% of the volume was recovered in the ultrafiltrate, containing the DOX unbound fraction. The Microcon-30 membranes were also rinsed and spun with 100 ul HCl (pH 2) in order to further elute membrane-bound DOX. Protein denaturation and precipitation was achieved by the addition of 70% perchloric acid (10 ul). Protein pellets were further extracted with 100 ul HCl (pH 2) to detect any DOX precipitation. More than 75% of DOX was recoverable using this method. The concentrations of DOX in the ultrafiltrate, retentate, protein pellet and Microcon-30 membrane wash were determined by HPLC.

**Pharmacokinetic Analysis.** Concentration-time curves C(t) were obtained by plotting the average data points from 3-5 animals. An inverse squared weighting scheme (MicroMath Scientist™ software) was utilized to fit the plasma concentration mean data based on the two-compartment model equation:

$$C(t) = A\, e^{-\alpha t} + B\, e^{-\beta t}$$

Initial estimates for A, B, α, β were obtained by residual analysis. Initial and terminal half-lives were calculated as $t_{1/2}(\alpha) = 0.693/\alpha$, and $t_{1/2}(\beta) = 0.693/\beta$.

The area under the plasma concentration-time curve (AUC, equivalent to $AUC_{0-\infty}$) and the total body clearance ($CL_t$) were calculated as follows:

$$AUC = A/\alpha + B/\beta$$

$$CL_t = \text{Dose} / AUC$$

The steady-state volume of distribution $V_{ss}$ was determined based on the standard methods for two-compartment analysis (Gibaldi and Perrier, 1982).

In addition, the method by Bailer (1988) was applied to statistically compare areas under the concentration-time curves from time zero to the last (24 hr) sampling time point ($AUC_{0-24}$). First, the mean $AUC_{0-24}$ was calculated using the linear trapezoidal method:

$$AUC_{0-24} = \sum_{i=2}^{m} C_i * \tfrac{1}{2} (\Delta t_{i-1} + \Delta t_i)$$

The variance and standard error of the AUC ($s^2_{AUC}$, $SE_{AUC}$) were then calculated based on:

$$s^2_{AUC} = \sum_{i=1}^{m} [\, \tfrac{1}{2} (t_i - t_{i-1})]^2 * [\, s^2_{Ci} / n_i]$$

$$SE_{AUC} = \sqrt{\; s^2_{AUC}}$$

The index variable i denotes the timepoint, i = 1, 2,…, m ($t_m$ = 24 h). The term $s^2_{Ci}$ denotes the variance of the plasma concentrations of $n_i$ animals at timepoint $t_i$.

The mean biliary and renal clearances ($CL_b$, $CL_r$) were calculated as:

$$CL_b = X_{bile(0\text{-}1h)} / AUC_{0\text{-}1h} \qquad CL_r = X_{u(0\text{-}24h)} / AUC_{0\text{-}24h}$$

$X_{bile(0\text{-}1h)}$ and $X_{u(0\text{-}24h)}$ denote the amounts of DOX excreted in bile and urine, respectively, for the indicated time intervals following administration of the drug. Since the metabolite levels in plasma were below detection limit at time points beyond 12 hrs, the $AUC_{0\text{-}12}$ was determined from the respective metabolite plasma profiles, and the renal clearances of the metabolites were calculated as: $CL_r = X_{u(0\text{-}12h)} / AUC_{0\text{-}12h}$

**Statistical Analysis.** Statistical analysis was performed using Student's t test (Microsoft Excel). Values of $p<0.05$ were considered significant.

For the statistical analysis of AUC values, the Z-test (Bailer, 1988) at a significance level of $\alpha=0.05$ was applied to compare mean AUC values between treatment groups, according to the test statistic:

$$Z = \frac{AUC_{\text{mean, Control}} - AUC_{\text{mean, LPS}}}{\sqrt{[s^2_{\text{AUC Control}} + s^2_{\text{AUC LPS}}]}}$$

An observed absolute Z value greater than the critical value of +1.96 was considered significant.

## RESULTS

**Hepatic and Renal P-glycoprotein Expression in Endotoxemia.** Induction of inflammation via administration of LPS resulted in a significant decrease of C-219 immunodetectable levels of PGP in the mice livers 24 h following treatment. Measured PGP protein levels in the liver of LPS-treated mice were 31 ± 13 % of that seen in control mice. In contrast, PGP protein levels in the kidneys of LPS-treated mice were found to be increased to 141 ± 12 % of control levels ($p<0.05$, Fig.1).

In the liver, LPS treatment resulted in significant ($p<0.05$) downregulation of *Mdr1a*, *Mdr1b*, *Mdr2* and *Bsep* mRNA levels (Fig. 2A). In the kidneys of LPS-treated mice levels of *Mdr1a* mRNA were unaltered whereas levels of *Mdr1b* mRNA were increased by two-fold as compared to controls ($p=0.06$, Fig. 2.B).

**Plasma Pharmacokinetics.** At time points up to 12 h, slightly higher plasma concentrations of DOX were found in LPS-treated mice, as compared to controls. The difference was most obvious during the early time period of 15 min to 2 h. At later time points (12 and 24 h), the plasma curves of control and LPS group coincided (Fig. 3). Table 1 lists the pharmacokinetic parameters calculated in both groups of mice. The AUC from time zero to 24 h was found to be significantly ($p<0.05$) higher in LPS-treated mice, although the relative increase in AUC was moderate (1.25-fold). The total clearance of DOX in LPS-treated animals was only slightly reduced by 8 % and the steady-state volume of distribution was ~78% of control values. The terminal half-life of DOX was similar in both groups (~18 h). In control animals, 35 % of the

drug was unbound in plasma, which is consistent with previous studies (Terasaki, 1984). A significant 60% decrease in DOX plasma protein binding was seen in plasma from LPS- treated mice ($p<0.001$).

Low plasma concentrations of the metabolites M2 (7-deoxy-doxorubicinone) and M3 (7-deoxy-doxorubicinolone) were detected up to 12 hrs following the administration of DOX (Fig.3B). While the $AUC_{0-12}$ for the metabolite M2 was five-fold higher in LPS-treated mice ($p<0.05$), the $AUC_{0-12}$ for M3 was somewhat lower (Table 2). M1 (doxorubicinol) could not be detected in plasma at the time points examined.

**Tissue Disposition.** Overall, the tissue disposition of DOX was similar in control and LPS-treated mice. The highest accumulation of drug was seen in liver and kidney (tissue/plasma ratios reached values up to ~500 for liver and kidney). In both groups, accumulation of DOX in the brain was only minor (with brain/plasma ratios of 2.3 to 2.6 at 8 h). For all tissues, maximal accumulation of DOX occurred at 8 h (Table 3).

The time course of tissue levels of DOX metabolites are summarized in Table 4. DOX metabolites were measurable in all tissues except for brain, where metabolite levels were below the limit of detection. In both control and LPS group, the highest metabolite levels in the liver were detected 1 h following administration of DOX, whereas in kidney and intestine the metabolites reached their maximum levels at 8 h. Normal and LPS-treated mice exhibited comparable hepatic levels of the metabolites M2 and M3 at 1 h and 8 h. By comparison, kidney levels of both M2 and M3 at most time points tended to be higher in LPS-treated mice. Intestinal

levels of M2 and M3 in LPS-treated mice were also found to be 2- to 3-fold increased ($p<0.05$) as compared to controls. While levels of M1 (doxorubicinol) was only detectable in the heart, we did not observe differences in M1 accumulation between LPS and control mice (Table 4).

**Biliary and Urinary Excretion.** LPS treatment did not significantly alter the bile flow (inset of Fig. 4.A). Bile flow in both groups occurred at an initial average rate of ~1.2 mg/min, then decreased to 0.6 mg/min and was stable up to 80 min at which time we concluded the experiment. Chromatographic analysis of bile samples revealed the presence of DOX and metabolite M3, whereby DOX accounted for about 99 % of recovered drug. In LPS-treated mice, we found that the cumulative amount of DOX excreted in bile over an 80-minute time period was significantly reduced by ~40 % as compared to controls (Fig. 4.A). The biliary clearance of DOX was significantly reduced in LPS-treated mice. Based on plasma values, we calculated a biliary clearance of $8.4 \pm 0.98$ mL/h in Control mice and $2.9 \pm 0.48$ mL/h in LPS-treated mice ($p<0.05$). Similarly, for the metabolite M3 we observed a reduction in biliary output by 50 % following LPS treatment (Fig. 5.B), and the biliary clearances for M3 were $2.3 \pm 0.55$ mL/h in Control mice and $0.76 \pm 0.14$ mL/h in LPS-treated mice ($p<0.05$).

Over a 24-hour time period, 1.7 % of the administered dose was recovered in the urine of Control animals as DOX and metabolites, with the parent drug accounting for more than 90 % of the recovered drug. The metabolites M1, M2 and M3 were also detected in urine, whereby M1 was predominant. As compared to controls, the amounts of unchanged DOX excreted in urine over the same time period was significantly increased by 3-fold (Fig. 4.B), and calculated renal clearances were 2.5-fold higher ($p<0.05$) in LPS-treated animals (Table 1). Moreover, while the

urinary excretion of M1 was unaltered upon LPS treatment, the amounts of M2 and M3 recovered in urine were increased by 5-fold and 2-fold, respectively ($p<0.05$ and $p=0.07$, Fig. 5.A). Whereas the renal clearance for M3 showed a slight trend of increase in LPS-treated versus control mice, no significant difference in the renal clearance for M2 was found between the two groups (Table 2). Total urine volume excreted over 24 h was the same for LPS-treated and Control mice.

## DISCUSSION

Our results demonstrate that endotoxin-induced inflammation can cause changes in the pharmacokinetics of the PGP substrate doxorubicin. These changes might partly be linked to altered PGP expression in liver and kidney. Differential regulatory mechanisms likely exist in these organs, resulting in suppression of hepatic PGP and upregulation of renal PGP. In other disease models, such as obstructive cholestasis in the rat, a similar adaptive regulation has been reported for the Multidrug Resistance Associated Protein, *Mrp2* (Lee et al., 2001). This tissue-specific response is thought to facilitate the removal of potentially toxic substances in disease states where the excretory capacity of the liver is diminished, but currently little is known regarding the molecular mechanisms. In the case of *Mrp2*, transcription factors such as the retinoid receptors RXR and RAR have been shown to play a role (Denson et al., 2002). More recent evidence also points towards the Pregnane X Receptor (PXR) and Constitutive Androstane Receptor (CAR), which are co-regulators of the *Mdr1a* and *Mdr1b* genes. PXR and CAR exhibit differential expression profiles in tissues (Maglich et al., 2002) and undergo downregulation during acute inflammation (Pascussi et al., 2000; Teng et al., 2004).

In our pharmacokinetic studies we found that LPS-induced inflammation caused an increase in the plasma-AUC but with only slight changes in the systemic clearance of DOX. Suppression of hepatic PGP would expectedly affect the systemic clearance of PGP substrates that undergo biliary elimination. However, our data shows that the impact of LPS on the systemic clearance of DOX is relatively moderate. This is not entirely surprising since multiple elimination pathways for DOX exist *in vivo*, and impairment of one pathway can compensated by increased

clearance through alternate routes. Reportedly direct intestinal secretion, which is not mediated by PGP, plays an important role in DOX clearance (Van Asperen, 2000). Our data demonstrates significantly greater amounts of DOX metabolites in the intestine of LPS-treated mice suggesting an increased intestinal clearance. DOX has a low hepatic extraction ratio of 0.2 (Ballet et al., 1987), thus changes in protein binding and intrinsic metabolic clearance could alter hepatic metabolism. Indeed, as plasma protein binding of DOX was decreased in LPS-treated mice, more free drug is accessible for hepatic metabolism. Thus, increased hepatic metabolic clearance could compensate for decreased biliary clearance, resulting in little change to total body clearance of DOX.

In our biliary excretion studies, we observed significant 50-65% decreases in both the biliary clearance of DOX and total amount excreted in bile. This is consistent with reports on the kinetics of DOX in rats with Shiga-like toxin-induced inflammation (Hidemura et al., 2003) and chronic inflammation, such as adjuvant arthritis (Achira et al., 2002). The corresponding downregulation in hepatic PGP expression clearly indicates that the decrease in functional PGP contributes to reduced biliary excretion of DOX. Since the C-219 antibody detects all *Mdr* isoforms (*Mdr1a, Mdr1b*, *Mdr2*) as well as *Bsep*, this raises the question whether the inflammation-mediated suppression affects specifically the drug-transporting PGP isoforms *Mdr1a* and *Mdr1b*. However we demonstrated through mRNA analysis that *Mdr1a* and *Mdr1b* expression is markedly suppressed, whereas *Mdr2* expression is reduced to a lesser extent.

In *Mdr1a*-deficient mice, an 80% decrease in DOX biliary output has been reported (Van Asperen et al., 2000), implying that *Mdr1a* is primarily responsible for the biliary excretion of

DOX. Interestingly, the cumulative amount of DOX excreted in bile during a 90-minute interval as reported by Van Asperen et al. (2000) (13% of dose) greatly exceeds our value (1.2% of dose). This discrepancy is likely due to differences in the technique of bile collection (gall bladder cannulation versus bile duct cannulation). The average bile flow rate in our mice was 0.6 mg/min, five times lower than the literature value of 3 mg/min (Bischoff et al., 1971) which suggests incomplete bile collection. This likely resulted in underestimation of DOX biliary excretion. When extrapolated to the expected bile flow rate, our biliary clearances were 52.3 mL/h (Control) and 14.9 mL/h (LPS). Reportedly, M1 (doxorubicinol) is effluxed into bile by PGP/*Mdr1a*, and a knockout of *Mdr1a* severely affects the biliary excretion of this metabolite (Van Asperen et al., 2000). Surprisingly, in our bile samples we detected M3 instead of M1, and the biliary excretion of M3 in endotoxin-induced inflammation was decreased to the same extent as that of DOX. This might imply either that M3 (but not M1) was extruded into the canalicular lumen by PGP, or that M1 underwent conversion to M3 immediately following entry into bile.

In our animal model of acute inflammation, we observed a 2.5 fold increase in renal clearance of DOX. The observed induction of PGP protein and *mdr1b* mRNA in the kidneys of LPS-treated mice likely exerts a prominent contribution to this finding. Our results are consistent with reports from *Mdr1a*/*1b* knockout mice indicating that functional impairment of hepatic PGP causes the excretion of PGP substrates to be shifted from the biliary to the renal route (Smit et al., 1998; Schinkel et al., 1997). Moreover, the decreased plasma protein binding of DOX in LPS-treated animals is likely to also contribute to increased urinary excretion. In addition, we cannot preclude the possibility that alternative mechanisms or carriers exist in the kidney, which may also be affected by LPS-treatment.

Interestingly, the increased unbound fraction of DOX in the plasma of LPS-treated mice was associated with decreased rather than increased steady-state distribution volume of DOX. Generally, while the initial distribution of DOX is rapid, extensive tissue accumulation occurs due to cell nuclei binding (Booth et al., 1998). Moreover, DOX distributes into erythrocytes with a typical blood:plasma concentration ratio of 2.4 (Terasaki et al., 1984). It is thus likely that the extent of tissue binding, or partitioning into erythrocytes is altered in LPS-treated mice. Indeed, DOX tissue levels were higher at 8 hr than at 1 hr after dosing, suggesting substantial tissue binding. Decreased PGP functional activity would be expected to result in drug accumulation in tissues that normally express PGP. For instance, Van Asperen et al. (1999) reported that *Mdr1a*-deficient mice exhibit 2- to 8-fold higher levels of DOX in liver, brain and small intestine. However, we did not detect significant differences in DOX accumulation in the LPS-treated animals. As numerous factors contribute to the distribution of DOX including blood flow, tissue binding and extra-hepatic metabolism; changes in any one or all of these factors by LPS treatment could obscure the impact on PGP mediated transport .

Decreased transporter functionality can alter the extent of metabolism for co-substrates of PGP and cytochrome P450 (Lau et al., 2004). Whether the same applies to non-P450 substrates such as DOX remains to be investigated. We collected greater amounts of M2 and M3 in the urine of LPS-treated mice. Given that renal clearance was not altered, this may imply an enhanced conversion of DOX to M2 and M3. Indeed, 5-fold higher amounts of M2 were observed in plasma and urine of LPS-treated mice. By comparison, the renal clearance of M3 appeared to be higher in LPS-treated mice. Hence, formation of M2 was likely increased in inflammation,

whereas for M3 an enhanced renal secretion (for instance, through induction of renal PGP) seems also plausible. Moreover, we found increased levels of M2 and M3 in intestine and kidney of LPS-treated mice. Thus, LPS treatment likely caused an increased formation of M2 and M3. Indeed, several enzymes involved in the reductive deglycosylation of DOX and doxorubicinol have been found to exhibit enhanced activity during inflammatory and hyperthermic conditions (Kan et al, 2004; Pfeffer et al, 1994; Dodion et al, 1986). We were able to detect M1 in urine but not in plasma, similar to previous reports (Van Asperen et al., 1999). M1 plasma levels are generally below detection limit due to its rapid clearance or sequential metabolism to M3. Hence it may not be possible to quantify M1 formation. It has been postulated that formation and intestinal clearance of M1 may be substantially underestimated due to enzymatic degradation in the gut (Van Asperen et al., 2000). One could also speculate that the metabolic clearance of DOX to M1 might be rate-limiting compared to the renal clearance of M1. Nevertheless, the possibility of increased formation of M1 in LPS-treated mice should not be excluded.

Overall, our findings suggest that acute inflammation causes differential regulation of PGP in liver and kidney, which enables the organism to sustain the elimination of PGP substrate drugs. Enhanced metabolism through selective pathways also occurs. Transporters in non-hepatic tissues can compensate for the loss of transporter function in the liver, the primary site of the acute inflammatory response. Thus, when predicting pharmacokinetics in disease states, it is crucial to consider alternate metabolic pathways. Furthermore, our findings highlight the importance of understanding the tissue-specific mechanisms of transporter and enzyme regulation.

**ACKNOWLEDGMENTS**

We thank Lichuan Liu for technical advice on the bile duct cannulation, and Stephen Mac and Martha Sobolev for their assistance with HPLC.

**REFERENCES**

Achira M, Totsuka R, Fujimura H and Kume T (2002) Tissue-specific regulation of expression and activity of P-glycoprotein in adjuvant arthritis rats. *Eur J Pharm Sci* **16:**29-36.

Bailer AJ (1988) Testing for the equality of area under the curves when using destructive measurement techniques. *J Pharmacokinet Biopharm* **16:**303-309.

Ballet F, Vrignaud P, Robert J, Rey C and Poupon R (1987) Hepatic extraction, metabolism and biliary excretion of doxorubicin in the isolated perfused rat liver. *Cancer Chemother Pharmacol* **19:**240-245.

Bischoff KB, Dedrick RL, Zaharko DS and Longstreth JA (1971) Methotrexate pharmacokinetics. *J Pharm Sci* **60:**1128-1133.

Booth CL, Brouwer KR, Brouwer KLR (1998) Effect of multidrug resistance modulators on the hepatobiliary disposition of doxorubicin in the isolated perfused rat liver. *Cancer Res* **38:**3641-3648.

Borst P and Schinkel AH (1997) Genetic dissection of the function of mammalian P-glycoproteins. *Trends Genet* **13:**217-222.

Broggini M, Colombo T, Martini A and Donelli MG (1980) Studies on the comparative distribution and biliary excretion of doxorubicin and 4'-epi-doxorubicin in mice and rats. *Cancer Treat Rep* **64:**897-904.

Decorti G, Peloso I, Favarin D, Klugmann FB, Candussio L, Crivellato E, Mallardi F and Baldini L (1998) Handling of doxorubicin by the LLC-PK1 kidney epithelial cell line. *J Pharmacol Exp Ther* **286:**525-530.

Denson LA, Bohan A, Held MA and Boyer JL (2002) Organ-specific alterations in RARalpha:RXRalpha abundance regulate rat *Mrp2* (Abcc2) expression in obstructive cholestasis. *Gastroenterology* **123:**599-607.

Dodion P, Riggs CE, Akman SR and Bachur NR (1986) Effect of hyperthermia on the in vivo metabolism of doxorubicin. *Cancer Treat Rep* **70:**625-629.

Gibaldi M and Perrier D (1982) Pharmacokinetics. 2nd ed. Marcel Dekker Inc., New York.

Goralski KB, Hartmann G, Piquette-Miller M and Renton KW (2003) Downregulation of *Mdr1a* expression in the brain and liver during CNS inflammation alters the in vivo disposition of digoxin. *Br J Pharmacol* **139:**35-48.

Hartmann G, Kim H and Piquette-Miller M (2001) Regulation of the hepatic multidrug resistance gene expression by endotoxin and inflammatory cytokines in mice. *Int Immunopharmacol* **1:**189-199.

Hidemura K, Zhao YL, Ito K, Nakao A, Tatsumi Y, Kanazawa H, Takagi K, Ohta M and Hasegawa T (2003) Shiga-like toxin II impairs hepatobiliary transport of doxorubicin in rats by down-regulation of hepatic P-glycoprotein and multidrug resistance-associated protein *Mrp2*. *Antimicrob Agents Chemother* **47:**1636-1642.

Kan W, Zhao KS, Jiang Y, Yan W, Huang Q, Wang J, Qin Q, Huang X and Wang S (2004) Lung, spleen, and kidney are the major places for inducible nitric oxide synthase expression in endotoxemic shock: role of p38 mitogen-activated protein kinase in signal transduction of inducible nitric oxide synthase expression. *Shock* **21:**281-287.

Kawaguchi H, Matsui Y, Watanabe Y and Takakura Y (2004) Effect of interferon-gamma on the pharmacokinetics of digoxin, a P-glycoprotein substrate, intravenously injected into the mouse. *J Pharmacol Exp Ther* **308:**91-96.

Lau YY, Wu CY, Okochi H and Benet LZ (2004) Ex situ inhibition of hepatic uptake and efflux significantly changes metabolism: hepatic enzyme-transporter interplay. *J Pharmacol Exp Ther* **308:**1040-1045.

Lee IK, Lee YM, Song IS, Chung SJ, Kim SG, Lee MG and Shim CK (2002) Hepatobiliary excretion of tributylmethylammonium in rats with lipopolysaccharide-induced acute inflammation. *Arch Pharm Res* **25:**969-72.

Lee J, Azzaroli F, Wang L, Soroka CJ, Gigliozzi A, Setchell KDR, Kramer W and Boyer JL (2001) Adaptive regulation of bile salt transporters in kidney and liver in obstructive cholestasis in the rat. *Gastroenterology* **121:**1473-1484.

Loveless H, Arena E, Felsted RL and Bachur NR (1978) Comparative mammalian metabolism of adriamycin and daunorubicin. *Cancer Res* **38:**593-598.

Maglich JM, Stoltz CM, Goodwin B, Hawkins-Brown D, Moore JT and Kliewer SA (2002) Nuclear Pregnane X Receptor and Constitutive Androstane Receptor regulate overlapping but distinct sets of genes involved in xenobiotic detoxification. *Mol Pharmacol* **62:**638-646.

Mayer LD and St.-Onge G (1995) Determination of Free and Liposome-Associated Doxorubicin and Vincristine Levels in Plasma under Equilibrium Conditions Employing Ultrafiltration Techniques. *Anal. Biochem.* **232:**149-157.

Pascussi JM, Gerbal-Chaloin S, Pichard-Garcia L, Daujat M, Fabre JM, Maurel P and Vilarem MJ (2000) Interleukin-6 negatively regulates the expression of Pregnane X Receptor and Constitutively Activated Receptor in human hepatocytes. *Biochem Biophys Res Commun* **274:**707-713.

Pfeffer KD, Huecksteadt TP and Hoidal JR (1994) Xanthine dehydrogenase and xanthine oxidase activity and gene expression in renal epithelial cells: cytokine and steroid regulation. *J Immunol* **153:**1789-1797.

Piquette-Miller M and Jamali F (1995) Influence of severity of inflammation on the disposition kinetics of propranolol enantiomers in ketoprofen-treated and untreated adjuvant arthritis. *Drug Metab Disp* **23:**240-245.

Piquette-Miller M, Pak A, Kim H, Anari R and Shahzamani A (1998) Decreased expression and activity of P-glycoprotein in rat liver during acute inflammation. *Pharm Res* **15:**706-711.

Schinkel AH, Mayer U, Wagenaar E, Mol AAM, van Deemter L, Smit JJM, van der Valk MA, Voordouw AC, Spits H, van Tellingen O, Zijlmans JMJM, Fibbe WE and Borst P (1997) Normal viability and altered pharmacokinetics in mice lacking mdr1-type (drug-transporting) P-glycoproteins. *Proc Nat Acad Sci USA* **94:**4028-4033.

Schneider RE and Bishop H (1982) Beta-blocker plasma concentrations and inflammatory disease: clinical implications. *Clin Pharmacokinet* **7:**281-284.

Smit JW, Schinkel AH, Weert B and Meijer DKF (1998) Hepatobiliary and intestinal clearance of amphiphilic cationic drugs in mice in which both *Mdr1a* and *Mdr1b* genes have been disrupted. *Br J Pharmacol* **124:**416-424.

Stride BD, Grant C, Loe DW, Hipfner DR, Cole SPC and Deeley RG (1997) Pharmacological characterization of the murine and human orthologs of multidrug-resistance protein in transfected human embryonic kidney cells. *Mol Pharmacol* **52:**344-353.

Takanashi S and Bachur NR (1976) Adriamycin metabolism in man: evidence from urinary metabolites. *Drug Metab Disp* **4:**79-87.

Teng S and Piquette-Miller M (2004) The involvement of PXR in hepatic gene regulation during inflammation in mice. *J Pharmacol Exp Ther,* 2005 ‘ in press’.

Terasaki T, Iga T, Sugiyama Y and Hanano M (1984) Pharmacokinetic study on the mechanism of tissue distribution of doxorubicin: interorgan and interspecies variation of tissue-to-plasma partition coefficients in rats, rabbits, and guinea pigs. *J Pharm Sci* **73:**1359-1363.

Trauner M, Meijer PJ and Boyer JL (1998) Molecular pathogenesis of cholestasis. *N Engl J Med* **339:**1217-1227.

Van Asperen J, Van Tellingen O and Beijnen JH (1998) Determination of doxorubicin and metabolites in murine specimens by high-performance liquid chromatography. *J Chromatogr B* **712:**129-143.

Van Asperen J, Van Tellingen O, Tijssen F, Schinkel AH and Beijnen JH (1999) Increased accumulation of doxorubicin and doxorubicinol in cardiac tissue of mice lacking *Mdr1a* P-glycoprotein. *Br J Cancer* **79:**108-113.

Van Asperen J, Van Tellingen O and Beijnen JH (2000) The role of mdr1a P-glycoprotein in the biliary and intestinal secretion of doxorubicin and vinblastine in mice. *Drug Metab Disp* **28:**264-267.

Footnotes

This study was funded by grants obtained from the Canadian Institute of Health Research.

Reprint Requests:

Micheline Piquette-Miller, PhD

Leslie Dan Faculty of Pharmacy,

144 College Street

Toronto, Ontario, Canada, M5S 3M2

**Legends for Figures**

**Figure 1. Effect of LPS-induced Inflammation on the Expression of Hepatic and Renal P-Glycoprotein.** Mice (n=4) were injected with saline buffer (Control) or 5 mg/kg i.p. LPS. Livers and kidneys were collected after 24 h. Immunodetectable levels of PGP were measured using C-219 antibody as described in Methods. Bars represent % mean values ± SEM of optical densities as compared to controls (*, $p<0.05$).

**Figure 2. Effect of LPS-induced Inflammation on the Expression of (A) Hepatic and (B) Renal *Mdr1* mRNA.** Mice (n=4) were injected with saline buffer (Control) or 5 mg/kg i.p. LPS. Livers and kidneys were collected after 6 h, and levels of *Mdr1a, Mdr1b, Mdr2* and *Bsep* mRNA were measured by RT-PCR as described in Methods. Bars represent % mean values ± SEM of 18S-normalized optical densities as compared to controls (*, $p<0.05$).

**Figure 3. Time Course of the Plasma Concentrations of A) Doxorubicin and (B) Metabolites in LPS and Control mice.** Mice (n=3-5 per time-point) were pre-treated with saline (Control, closed symbols) or 5 mg/kg i.p. endotoxin (LPS, open symbols), and received 5 mg/kg i.v. DOX 24 h following treatment. Data points represent mean ± SE. (*, $p<0.05$)

**Figure 4. Effect of LPS-induced Inflammation on the Cumulative Excretion of Doxorubicin into (A) Bile and (B) Urine.** Mice (n=5) were pre-treated with saline (Control) or 5 mg/kg i.p. LPS, and received 5 mg/kg i.v. DOX 24 h following treatment. Bile flow (inset), biliary excretion, and urinary excretion of DOX was measured as described in Methods. Data points represent mean ± SEM. Absence of error bars indicates that the SEM is smaller than the size of the symbols. (*, $p<0.05$)

**Figure 5. Effect of LPS-induced Inflammation on the Cumulative Excretion of DOX Metabolites into (A) Urine and (B) Bile.** Mice (n=5) were pre-treated with saline (Control) or 5 mg/kg i.p. LPS, and received 5 mg/kg i.v. DOX 24 h following treatment. Biliary and urinary excretion of metabolites was measured as described in Methods. Bars represent mean ± SEM. (*, $p<0.05$)

DMD Fast Forward. Published on March 18, 2005 as DOI: 10.1124/dmd.104.002568
This article has not been copyedited and formatted. The final version may differ from this version.



## TABLES

**Table 1.** Pharmacokinetic parameters of doxorubicin in plasma of control versus LPS-treated mice following a 5 mg/kg i.v. dose (mean ± SE).

| | Control | LPS |
|---|---|---|
| $AUC_{0-24}$, (ng*h)/mL [a] | 609.0 ± 42.0 | * 771.6 ± 40.7 |
| $CL_t$, mL/h [b] | 139.7 | 128.9 |
| $f_{u,\ plasma}$ [c] | 0.35 ± 0.004 | * 0.67 ± 0.006 |
| $t_{½}$ (β), h [d] | 18.3 | 17.8 |
| $V_{ss}$, mL [e] | 3249 | 2531 |
| $CL_r$, mL/h [f] | 4.05 ±0 .28 | * 10.3 ± 0.54 |

[a] Mean and SE of $AUC_{0-24}$ calculated using Bailer's method.
* : significantly different from controls, $p<0.05$ (Z test).
[b] $CL_t$ calculated by compartmental analysis as Dose/$AUC_{0-\infty}$.
[c] determined at plasma concentration 100 ng/mL.
[d] $t_{½}$ (β) calculated as 0.693/β.
[e] $V_{ss}$ calculated by compartmental analysis as $V_1 + V_2$.
[f] $CL_r$ calculated by $\Sigma Xu_{24}/AUC_{24}$.

DMD Fast Forward. Published on March 18, 2005 as DOI: 10.1124/dmd.104.002568
This article has not been copyedited and formatted. The final version may differ from this version.



**Table 2.** Pharmacokinetic parameters of doxorubicin metabolites in plasma of control versus LPS-treated mice following administration of doxorubicin at a 5 mg/kg i.v. dose (mean ± SE).

| | M2 (7-deoxy-doxorubicinone) | | M3 (7-deoxy-doxorubicinolone) | |
|---|---|---|---|---|
| | Control | LPS | Control | LPS |
| $AUC_{0\text{-}12}$, (ng*h)/mL | 53.0 ± 8.6 | * 263.3 ± 62.8 | 131.6 ± 28.3 | 98.5 ± 14.7 |
| $CL_r$, mL/h | 0.31 ± 0.05 | 0.35 ± 0.08 | 0.25 ± 0.05 | 0.53 ± 0.08 |

* : significantly different from controls, $p<0.05$ (Z test).
n.d.: not detectable.

DMD Fast Forward. Published on March 18, 2005 as DOI: 10.1124/dmd.104.002568
This article has not been copyedited and formatted. The final version may differ from this version.



**Table 3.** Time course of doxorubicin tissue levels in control versus LPS-treated mice following a 5 mg/kg i.v. dose, expressed as tissue-to-plasma ratios in ml/g (mean ± SEM, n=5).

| | 1 h | | 8 h | | 24 h | |
|---|---|---|---|---|---|---|
| | Control | LPS | Control | LPS | Control | LPS |
| Liver | 176 ± 45 | 226 ± 106 | 510 ± 66 | 531 ± 34 | 210 ± 20 | 181 ± 8 |
| Kidney | 160 ± 55 | 133 ± 90 | 485 ± 69 | 325 ± 40 | 278 ± 67 | 268 ± 39 |
| Brain | 0.3 ± 0.05 | 0.2 ± 0.01 | 2.3 ± 0.6 | 2.6 ± 0.2 | < 0.1 | < 0.1 |
| Intestine | 15 ± 5.7 | 16 ± 11 | 66 ± 20 | 53 ± 9.5 | 30 ± 3.5 | 31 ± 5.5 |
| Heart | 35 ± 7 | 36 ± 19 | 102 ± 15 | 98 ± 24 | n.d. | n.d. |

n.d.: not detectable

DMD Fast Forward. Published on March 18, 2005 as DOI: 10.1124/dmd.104.002568
This article has not been copyedited and formatted. The final version may differ from this version.



**Table 4.** Time course of doxorubicin metabolite tissue levels in control versus LPS-treated mice following administration of doxorubicin at a 5 mg/kg i.v. dose (mean ± SEM).

| | | 1 h | | 8 h | |
|---|---|---|---|---|---|
| | | Control | LPS | Control | LPS |
| Liver | M2 | 1170 ± 872 | 1170 ± 183 | 307 ± 58 | 332 ± 50 |
| | M3 | 1096 ± 946 | 1428 ± 340 | 340 ± 83 | 307 ± 91 |
| Kidney | M2 | 22 ± 13 | 33 ± 15 | 30 ± 11 | * 101 ± 28 |
| | M3 | 521 ± 50 | * 785 ± 83 | 159 ± 34 | 208 ± 116 |
| Intestine | M2 | 374 ± 100 | 340 ± 91 | 863 ± 257 | * 2706 ± 506 |
| | M3 | n.d. | n.d. | 432 ± 108 | * 905 ± 108 |
| Heart | M1 | n.d. | n.d. | 87 ± 34 | 95 ± 34 |

Numbers represent mean ± SEM (n=5) of absolute amounts in ng DOX equivalents per g of tissue. * : significantly different from controls, $p<0.05$. n.d.: not detectable.

DMD Fast Forward. Published on March 18, 2005 as DOI: 10.1124/dmd.104.002568
This article has not been copyedited and formatted. The final version may differ from this version.

Figure 1

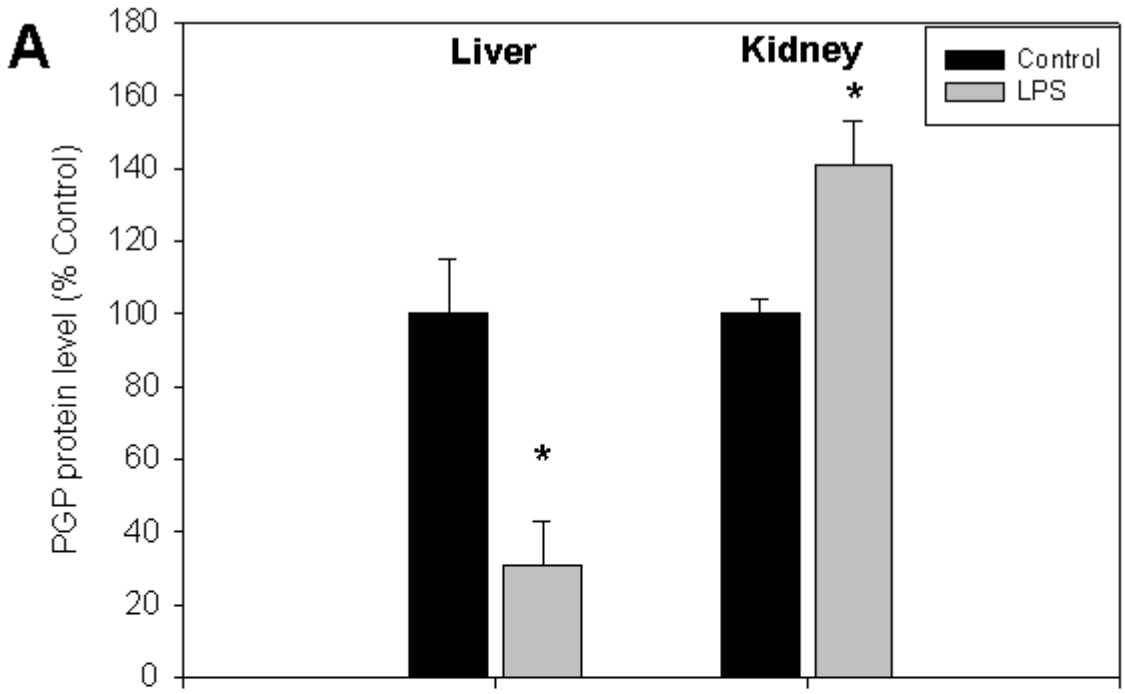


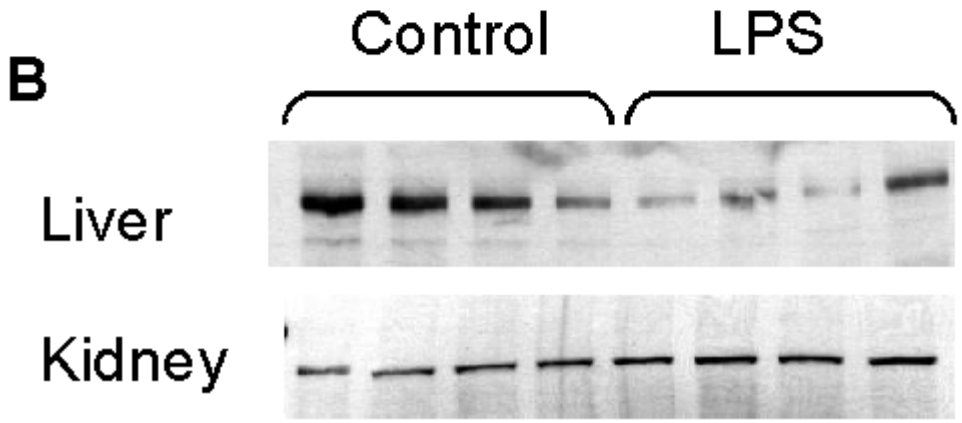

DMD Fast Forward. Published on March 18, 2005 as DOI: 10.1124/dmd.104.002568
This article has not been copyedited and formatted. The final version may differ from this version.

Figure 2

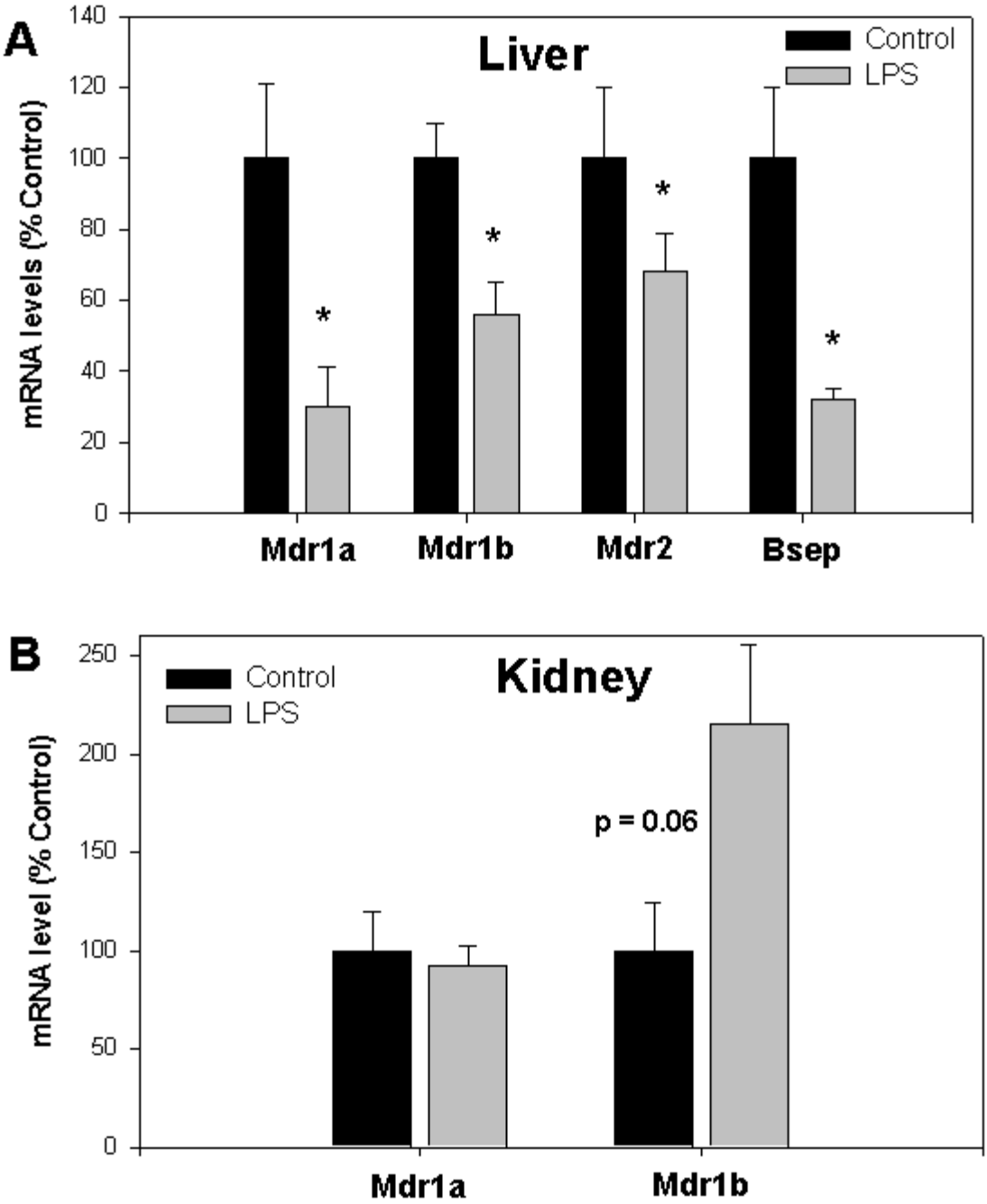

DMD Fast Forward. Published on March 18, 2005 as DOI: 10.1124/dmd.104.002568


# Figure 3

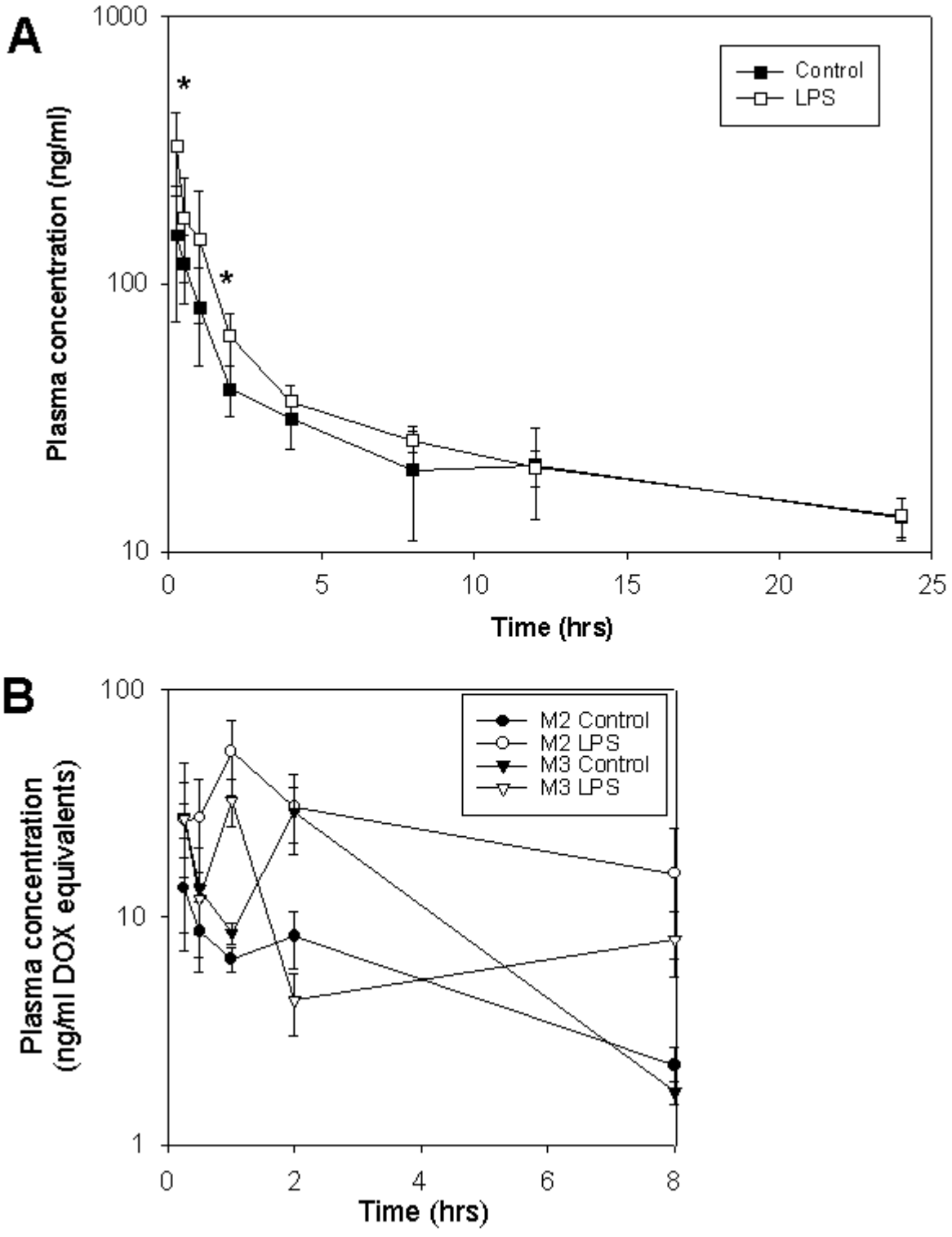

DMD Fast Forward. Published on March 18, 2005 as DOI: 10.1124/dmd.104.002568
This article has not been copyedited and formatted. The final version may differ from this version.

# Figure 4

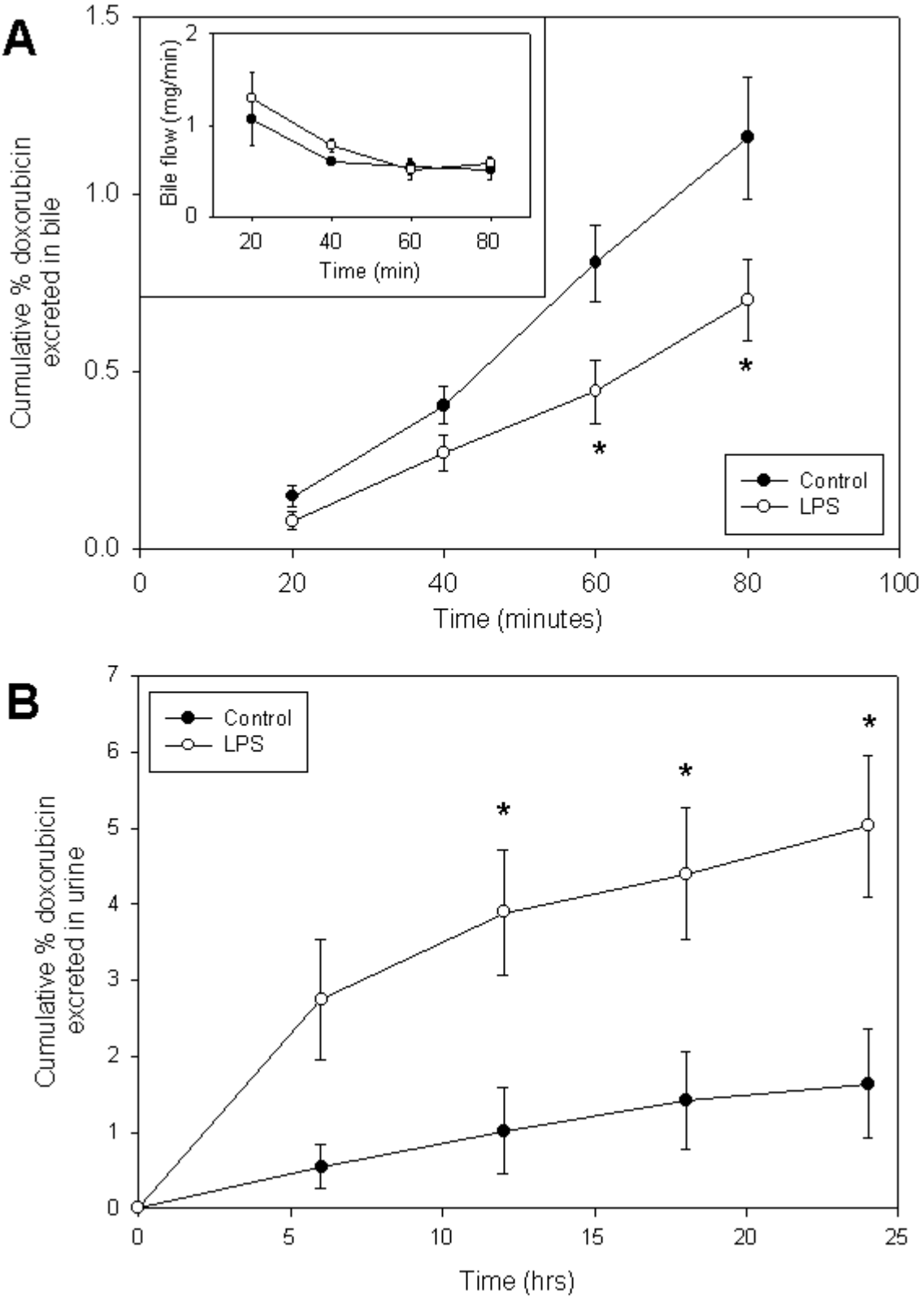

DMD Fast Forward. Published on March 18, 2005 as DOI: 10.1124/dmd.104.002568


# Figure 5